# Active cloaking of rigid and elastic cylindrical scatterers

**Daniel Eggler (1), Hyuck Chung (2), Fabien Montiel (3), Jie Pan (4) and Nicole Kessissoglou (1)**

(1) School of Mechanical and Manufacturing Engineering, The University of New South Wales, Australia
(2) School of Computer and Mathematical Sciences, Auckland University of Technology, New Zealand
(3) Department of Mathematics & Statistics, University of Otago, New Zealand
(4) School of Mechanical and Chemical Engineering, The University of Western Australia, Australia

## ABSTRACT

This work presents active cloaking of rigid and elastic cylindrical shells. The acoustic performance using single and multiple control sources and error sensors is investigated for different control configurations. Scattering by a rigid cylinder due to an incident plane wave is initially studied. The scattered acoustic field is actively attenuated using monopole control sources and error sensors located circumferentially around the cylinder. The structural and acoustic responses of an elastic shell due to an incident plane wave are then examined. Active cloaking at the shell circumferential modes is achieved using monopole control sources located in the surrounding fluid. Active structural acoustic cloaking is also achieved using control forces applied directly to the shell.

## 1   INTRODUCTION

The ability to remove the presence of an object from detection was considered the realm of science fiction until Pendry et al. (2006) detailed a method for theoretically controlling electromagnetic (EM) waves using optical conformal mapping. This heralded the beginning of cloaking metamaterials whereby the metamaterial is able to guide the incident field around the object. There has been considerable work on passive cloaking across a range of different fields including acoustics, optics and elastic waves, for example, see Milton et al. (2006), Farhat et al. (2009), Norris (2008), Zigoneanu et al. (2014), although the list is by no means exhaustive. Each cloak must be designed for a specific set of conditions; any deviation from the expected incident field requires the cloak to be redesigned. Active cloaking utilises active sources to suppress the scattered field generated by an object (Vasquez et al. 2009a, 2009b). In early work, Friot and Bordier (2004) analytically and experimentally investigated real-time suppression of the scattered field generated by an object. Despite being ahead of its time, research on active cloaking remained dormant until there was a surge in interest in passive methods for cloaking. In recent years active cloaks have been proposed in acoustics (Vasquez et al. 2009a, 2009b, 2011), elastic waves (Futhazar et al. 2015; Norris et al. 2014; O'Neill et al. 2015; O'Neill et al. 2016) and optics (Miller 2006).

This paper investigates acoustic cloaking of both rigid and elastic cylindrical scatterers under incident plane excitation using conventional active noise control techniques. An idealised application of this work is to avoid detection of an underwater vehicle by active sonar. A single scatterer in an infinite acoustic medium is considered. The rigid cylinder is actively cloaked using monopole control sources located circumferentially around the cylinder. The scattered field due to an incident plane wave is actively attenuated at error microphone locations, also located circumferentially around the cylinder. The structural and acoustic responses of an elastic cylinder are then investigated. Similar to the rigid scatterer case, active noise control (ANC) using monopole control sources located circumferentially around the elastic cylindrical shell are used to cloak the shell at its first three circumferential modes. Active structural acoustic cloaking (ASACL) using point control forces applied directly to the elastic shell are also implemented, for the first time, to cloak the shell at its circumferential modes.

## 2   ANALYTICAL METHODOLOGY

### 2.1  Rigid cylinder

The solution to the scattering from an infinitely long rigid cylinder impinged by an incident plane wave is well known and a concise summary is provided by Martin (2006). The following equations respectively represent separated solutions to the Helmholtz equation in plane polar coordinates for the incident and scattered pressure

$$p_{\text{inc}}(r,\theta) = \sum_{n=-\infty}^{\infty} \mathrm{i}^n J_n(kr) e^{\mathrm{i}n\theta}, \qquad p_{\text{sc}}(r,\theta) = -\sum_{n=-\infty}^{\infty} \mathrm{i}^n \frac{J_n'(ka)}{H_n'(ka)} H_n(kr) e^{\mathrm{i}n\theta} \qquad (1,2)$$

where i is the imaginary number, $J_n$ is the Bessel function and $H_n$ is the Hankel function, both of the first kind of order $n$, ' denotes the spatial derivative, $k$ is the acoustic wavenumber given by $\omega/c$, $\omega$ is the angular frequency and $c$ is the speed of sound.

## 2.2 Elastic cylindrical shell

For the case of an infinitely long elastic cylindrical shell, only the radial and tangential shell displacements, denoted by $w$ and $v$, respectively, are considered. The equations of motion for the radial and tangential shell displacements are given by

$$D \frac{d^4}{d\theta^4} w(\theta) + D\beta^2 w(\theta) - m\omega^2 w(\theta) + D\beta^2 \frac{d}{d\theta} v(\theta) = p_{\text{int}}(a,\theta) - p_{\text{ext}}(a,\theta) \tag{3}$$

$$G \frac{d}{d\theta} w(\theta) + G \frac{d^2}{d\theta^2} v(\theta) + m\omega^2 v(\theta) = 0 \tag{4}$$

where $(r,\theta)$ represents the field point in polar coordinates, $r$ is the distance from the centre of the scatterer to the field point, and $\theta$ is the angle from the horizontal axis to the field point. $D$ is the flexural rigidity, $\beta = \sqrt{12}(a/h)$ is the shell thickness parameter, $G$ is the shear modulus, $m = \rho h$, $a$ is the cylinder radius at its midplane thickness, $\rho$ is the shell density and $h$ is the shell thickness. $p_{\text{int}}(a,\theta)$ and $p_{\text{ext}}(a,\theta)$ are the acoustic pressures on the interior and exterior shell surfaces, respectively. Fourier series are used to represent the shell radial and tangential displacement functions as follows

$$w(\theta) = \sum_{n=-\infty}^{\infty} w_n e^{in\theta}, \qquad v(\theta) = \sum_{n=-\infty}^{\infty} v_n e^{in\theta} \tag{5,6}$$

The pressure field is computed by solving the Helmholtz and elastic thin shell equations that are coupled by the kinematic conditions on both the interior and exterior surfaces of the shell. The external and internal pressure fields of the cylindrical shell can be expressed as (Chung et al. 2017)

$$p_{\text{ext}}(r,\theta) = \sum_{n=-\infty}^{\infty} \left( a_n \frac{J_n(kr)}{J_n'(ka)} + b_n \frac{H_n(kr)}{H_n'(ka)} \right) e^{in\theta} \tag{7}$$

$$p_{\text{int}}(r,\theta) = \sum_{n=-\infty}^{\infty} c_n \frac{J_n(kr)}{J_n'(ka)} e^{in\theta} \tag{8}$$

where $a_n$ is the known coefficient related to the incident field, $b_n$ is the coefficient related to the scattered and radiated external pressure field due to incident wave excitation and $c_n$ is the coefficient for the internal field. The unknown amplitudes $b_n$, $c_n$, $w_n$ and $v_n$ are obtained for an arbitrary incident field using a standard mode matching technique (Chung et al. 2017).

## 3 ACTIVE CONTROL

The control approach is based on the feedforward adaptive least-mean-square algorithm (Widrow and Stearns 1985). The cost function is the sum of the squares of the acoustic pressure at field points corresponding to error sensor locations. Using multiple control sources and multiple error sensors, the cost function is given by (Keir et al. 2005)

$$pp^* = \sum_{e=1}^{l} \left( \left( p_p G_p(r_e,\theta_e) + \sum_{j=1}^{N} p_{s,j} G_{s,j}(r_e,\theta_e) \right) \left( p_p G_p(r_e,\theta_e) + \sum_{j=1}^{N} p_{s,j} G_{s,j}(r_e,\theta_e) \right)^* \right) \tag{9}$$

where $()^*$ is the complex conjugate $p_p$ is the incident plane wave amplitude, $G_p$ is the primary transfer function of the acoustic response associated with the incident plane wave, $G_{s,j}$ is the secondary transfer function of the acoustic response associated with the $j$th control source and $p_{s,j}$ is the $j$th control source amplitude. A total of $N$ control sources were considered. The subscript $e$ denotes the error sensor at location $(r_e,\theta_e)$ with a total of $l$ error sensors considered. The optimal control source amplitudes were obtained by partially differentiating the cost function with respect to the real and imaginary components of the control sources and equating to zero.

For active cloaking of the rigid and elastic cylinders, the incident field is removed from the cost function given by eq. (9). For the rigid cylinder case, $G_p$ corresponds to the scattered pressure $p_{sc}$ given by eq. (2) and similarly, for the elastic cylinder case, $G_p$ is given by the second term on the right hand side of eq. (7) corresponding to the scattered and radiated pressure due to the incident field. $G_s$ is the total acoustic pressure due to the monopole sources (for the rigid cylinder case) or due to the point forces (for the elastic cylinder case using active structural acoustic cloaking).

## 4    CONTROL ARRANGEMENT

An infinitely long cylindrical scatterer in an infinite acoustic medium is considered. The fluid medium is air with sound speed of 343 m/s and density of 1.225 kg/m$^3$. The elastic shell has a thickness of 3 mm, density 1300 kg/m$^3$, Young's modulus 2.9 GPa and Poisson's ratio of 0.3. The cylinder radius is $a$ = 0.6 m. For the rigid cylinder case, active cloaking was implemented using monopole sources and error sensors arranged circumferentially around the cylinder, as shown in Figure 1a. The monopole sources were located at $2a$ from the centre of the cylinder and the error sensors were located at $3a$ from the cylinder centre. For the elastic cylinder case, active cloaking was implemented by attenuating the external scattered and radiated acoustic field due to the incident plane wave as represented by the second term of the right hand side of eq. (7). The second control configuration using point forces applied directly to the shell, as shown in Figure 1b, was also considered. This second control arrangement is more commonly termed active structural acoustic control (ASAC). For both control arrangements shown in Figure 1, an equal number of control sources and error sensor were used, with the first control source or point force always at $\theta = 0$. All control sources and error sensors were equally spaced in the circumferential direction.
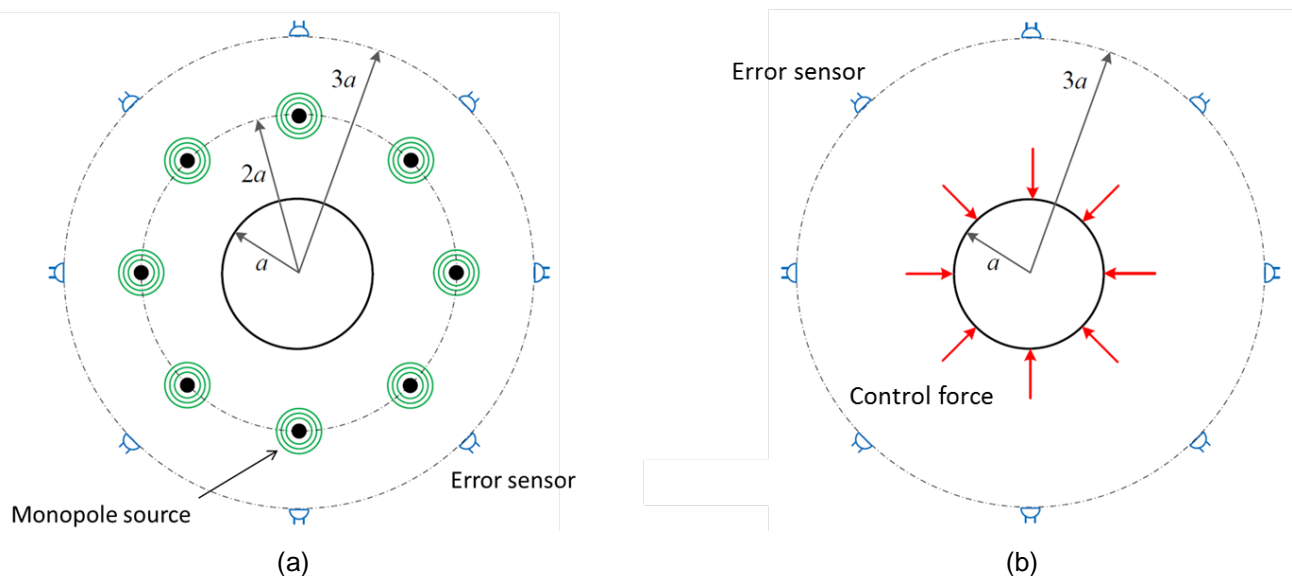


Figure 1 - Control arrangement using (a) monopole sources and (b) point forces

## 5    RESULTS

### 5.1  Rigid cylinder

Results are initially presented for a rigid scatterer under plane wave excitation whereby the plane wave is travelling from left to right. Figure 2 presents the acoustic pressure field of an incident plane wave at 278 Hz (Figure 2a), the acoustic field due to scattering by a rigid cylinder (Figure 2b) and the acoustic field after active noise control was implemented to attenuate the scattered field only (Figure 2c). Active control was implemented using 15 monopole control sources and 15 error sensors. The controlled field in Figure 2c shows excellent cloaking of the scatterer with the exception of the fluid region between the control sources and cylinder, whereby the actively controlled acoustic field resembles the incident field in Figure 2a.

Figure 3 presents the directivity, corresponding here to the absolute acoustic pressure, of the acoustic pressure field at a distance of $3a$ from the centre of the cylinder. Figure 3a shows the directivity of the incident field at 278 Hz, Figure 3b presents the directivity of the acoustic field due to scattering by the rigid cylinder, and Figure 3c presents the directivity of the cloaked field. Figure 3c indicates cloaking can be improved, which can be achieved by increasing the number of error sensors and possibly the number of control sources.
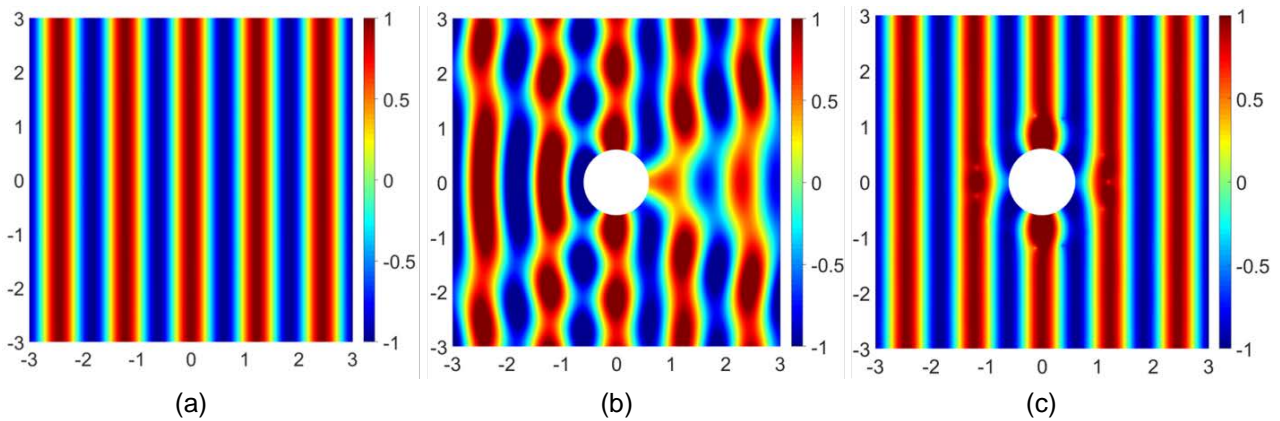
Figure 2 - Acoustic pressure field under incident plane wave excitation (a) in the absence of a rigid scatterer, (b) with a rigid scatterer and (c) actively cloaked with 15 control sources.
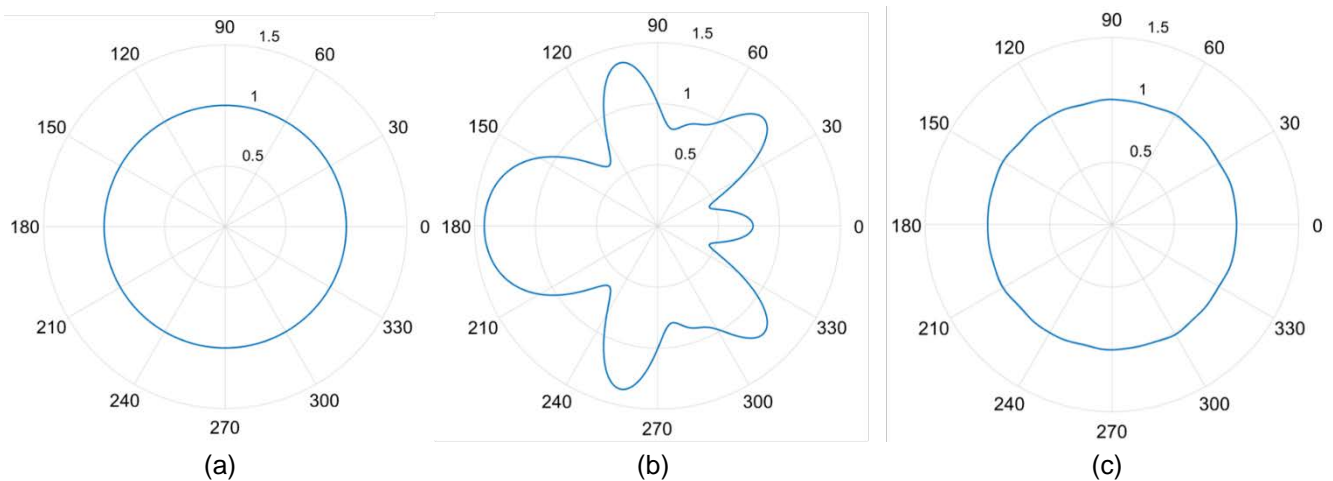


Figure 3 – Directivity of acoustic pressure field under incident plane wave excitation (a) in the absence of a rigid scatterer, (b) with a rigid scatterer and (c) actively cloaked with 15 control sources.

## 5.2 Elastic cylindrical shell

Results for an elastic cylindrical shell are now presented. The acoustic pressure of the elastic scatterer under plane wave, single monopole source and single point force excitation was initially examined at an error microphone location downstream of the shell. Although not shown here, the acoustic pressure as a function of frequency for the three excitation cases revealed three peaks at 167.1 Hz, 278.1 Hz and 384.5 Hz. These frequencies correspond to the first three circumferential modes of the shell (noting that the lowest order accordion circumferential shell mode cannot be excited for the excitation cases considered here). The acoustic field and corresponding shell deformation of the elastic shell under plane wave excitation at each of the frequencies are shown in Figure 4a, Figure 5a and Figure 6a. Similar to the rigid cylinder case, the plane wave is travelling from left to right. In Figure 4a, bending motion at the $n = 1$ circumferential mode in the direction of the incident plane wave propagation is clearly visible, where $n$ is the shell circumferential mode number. Similarly, in Figure 5a, the ovalling motion of the shell corresponding to the $n = 2$ circumferential mode is shown, and at 384.5 Hz in Figure 6a, the $n = 3$ circumferential mode of the shell can be observed. Active cloaking using monopole control sources located circumferentially around the shell is shown in Figure 4b, Figure 5b and Figure 6b, whilst active cloaking using point control forces applied to the shell are shown in Figure 4c, Figure 5c and Figure 6c. The control configuration in all results comprises 16 control sources or forces and 16 error sensors, with the exception of the results in Figure 6b. At 384.5 Hz, 16 monopole sources and 16 error sensors were insufficient to achieve effective cloaking and hence the number of monopole sources and error sensors was doubled. For active structural acoustic cloaking (ASACL), the number of point control forces required for effective cloaking is significantly reduced due to the fact that the control forces are in closer proximity to each other. Active cloaking using monopole control sources is achieved in the acoustic field external to the location of the monopole sources. It is inter-

esting to observe that for active cloaking using point control forces, acoustic cloaking is achieved both in the internal and external fluid regions, attributed to the fact that the point forces are applied directly to the shell which in turn directly couples with the internal and external fluids. The shell deformation with the implementation of ASACL can also be observed.

## 6  CONCLUSIONS

Rigid and elastic cylinders under incident plane wave excitation were acoustically cloaked using conventional active noise control methods. Utilising monopole control sources and error sensors located circumferentially around the scatterer, the rigid cylinder was cloaked by actively attenuating the scattered field, whereby the resulting acoustic field resembled the incident field. The elastic cylinder was actively cloaked at the first three circumferential shell modes using both ANC and ASAC approaches, whereby the ANC approach utilises monopole sources and error sensors in the external fluid, and the ASAC approach replaces the monopole sources with point forces applied radially to directly excite the shell. For the latter case of active structural acoustic cloaking, both the internal and external fluid fields were actively cloaked. Furthermore, the required number of point control forces compared to the number of monopole control sources is significantly reduced due to the fact that the point forces are in closer proximity to each other. In this work, the number of control sources and error sensors were arbitrarily chosen. Current work is underway to select the optimal number of control sources and error sensors to achieve acoustic cloaking with minimum control effort. Future work will examine the effect of a heavy fluid medium on the active control performance, in particular, for an elastic shell submerged in water whereby the heavy fluid becomes fully coupled with the shell displacements.

## REFERENCES

Chung, H., Montiel, F., Karimi, M. and Kessissoglou, N. 2017. 'Acoustic pressure fields of 2D elastic cylindrical shells'. In *Proceedings of the 46th International Congress and Exposition on Noise Control Engineering (Inter-Noise 2017)*, Hong Kong.

Farhat, M., Guenneau, S. and Enoch, S. 2009. 'Ultrabroadband elastic cloaking in thin plates'. *Physical Review Letters* 103 (2): 024301.

Friot, E. and Bordier, C. 2004. 'Real-time active suppression of scattered acoustic radiation'. *Journal of Sound and Vibration* 278 (3): 563-580.

Futhazar, G., Parnell, W. and Norris, A.N. 2015. 'Active cloaking of flexural waves in thin plates'. *Journal of Sound and Vibration* 356:1-19.

Keir, J., Kessissoglou, N. and Norwood, C. 2005. 'Active control of connected plates using single and multiple actuators and error sensors'. *Journal of Sound and Vibration* 281 (1): 73-97.

Martin, P. 2006. '*Multiple scattering: Interaction of time-harmonic waves with N obstacles*', Cambridge University Press.

Miller, D. 2006. 'On perfect cloaking'. *Optics Express* 14 (25): 12457-12466.

Milton, G.W., Briane, M. and Willis, J.R. 2006. 'On cloaking for elasticity and physical equations with a transformation invariant form'. *New Journal of Physics* 8 (10): 248-248.

Norris, A.N. 2008. 'Acoustic cloaking in 2D and 3D using finite mass'. arXiv preprint. arXiv:0802.0701.

Norris, A.N., Amirkulova, F. and Parnell, W. 2014. 'Active elastodynamic cloaking'. *Mathematics and Mechanics of Solids* 19 (6): 603-625.

O'Neill, J., Selsil, Ö., McPhedran, R.C., Movchan, A.B. and Movchan, N.V. 2015. 'Active cloaking of inclusions for flexural waves in thin elastic plates'. *The Quarterly Journal of Mechanics and Applied Mathematics* 68 (3): 263-288.

O'Neill, J., Selsil, Ö., McPhedran, R.C., Movchan, A.B., Movchan, N.V. and Henderson Moggach, C. 2016. 'Active cloaking of resonant coated inclusions for waves in membranes and Kirchhoff plates'. *The Quarterly Journal of Mechanics and Applied Mathematics* 69 (2): 115-159.

Pendry, J., Schurig, D. and Smith, D. 2006. 'Controlling electromagnetic fields'. *Science* 312 (5781): 1780-1782.

Vasquez, F., Milton, G. and Onofrei, D. 2009a. 'Active exterior cloaking for the 2D Laplace and Helmholtz equations'. *Physical Review Letters* 103 (7): 073901.

Vasquez, F., Milton, G. and Onofrei, D. 2009b. 'Broadband exterior cloaking'. *Optics Express* 17 (17): 14800-14805.

Vasquez, F., Milton, G. and Onofrei, D. 2011. 'Exterior cloaking with active sources in two dimensional acoustics'. *Wave Motion* 48 (6): 515-524.

Widrow, B. and Stearns, S. 1985. '*Adaptive signal processing*'. Englewood Cliffs, Prentice-Hall.

Zigoneanu, L., Popa, B.I. and Cummer, S. 2014. 'Three-dimensional broadband omnidirectional acoustic ground cloak'. *Nature Materials* 13 (4): 352-355.
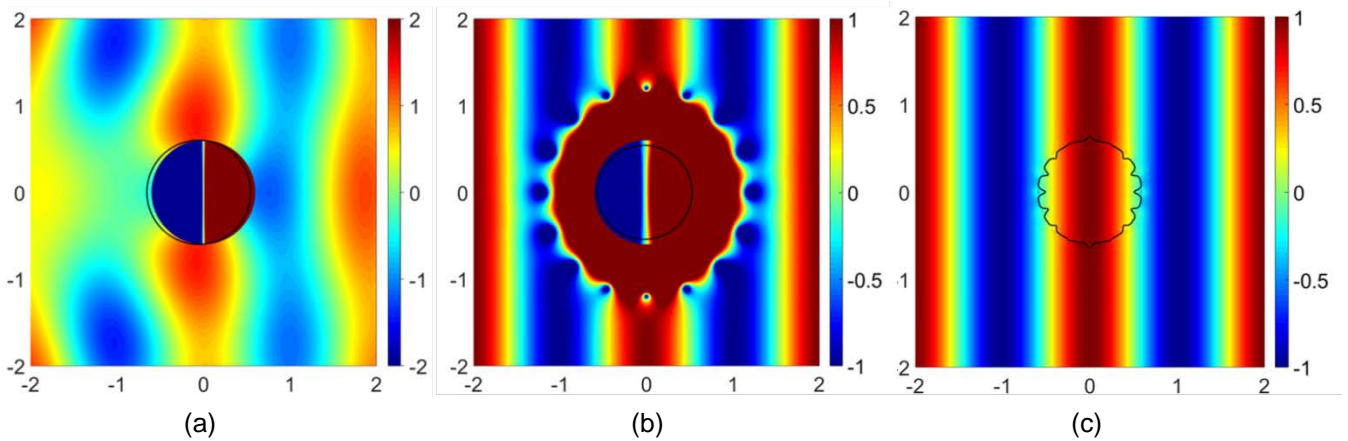
Figure 4 – (a) Acoustic pressure field and shell deformation under plane wave excitation at 167.1 Hz, (b) active cloaking using ANC, (c) active cloaking using ASACL.
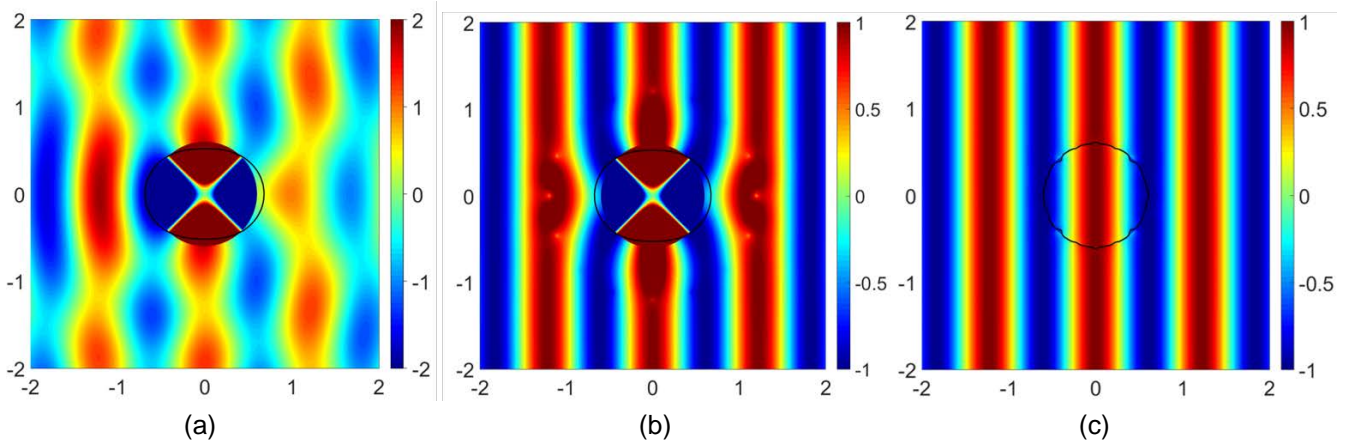


Figure 5 - (a) Acoustic pressure field and shell deformation under plane wave excitation at 278.1 Hz, (b) active cloaking using ANC, (c) active cloaking using ASACL.
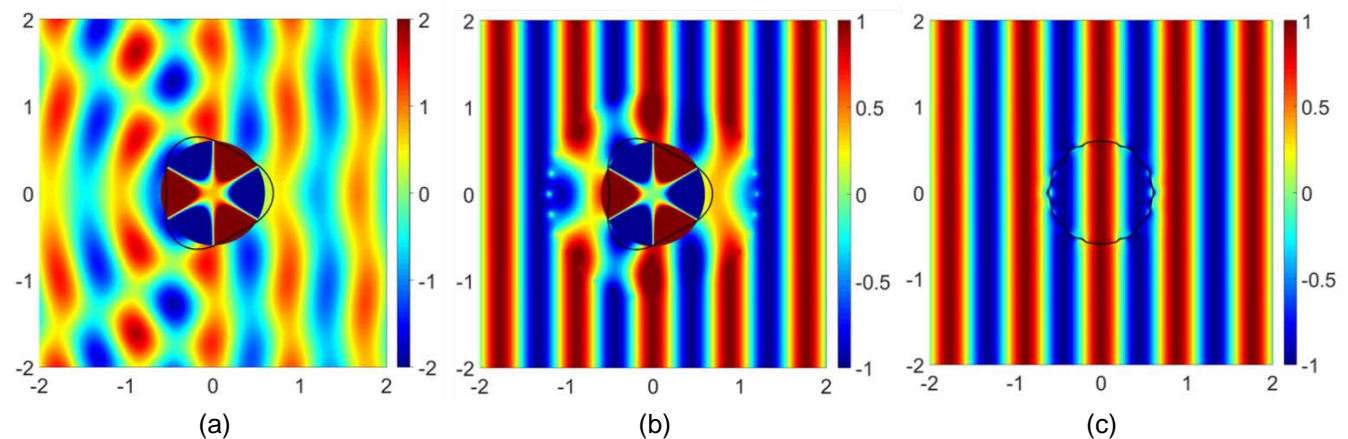


Figure 6 – (a) Acoustic pressure field and shell deformation under plane wave excitation at 384.5 Hz, (b) active cloaking using ANC, (c) active cloaking using ASACL.